Efficient Transfer Hydrogenation of Furfural via F Doping in Mesoporous ZrO_2

Beibei Gao[a], Jongbok Choi[b*], Ziling Zhang[a], Yuqing Luo[a], Barun Li[a], Lianjun Wang[a], Wan Jiang[a], Pengpeng Qiu [a*], and Wei Luo[a*]

[a]State Key Laboratory for Modification of Chemical Fibers and Polymer Materials, College of Materials Science and Engineering, Donghua University, Shanghai 201620, China.

[b]School of Chemistry, Faculty of Science, University of Melbourne, VIC 3010, Australia

[*]Corresponding authors.

E-mail addresses: choijongbok42@gmail.com, qiupengpeng@dhu.edu.cn (P. Qiu), wluo@dhu.edu.cn (W. Luo).

Experimental section

Materials

F127 ($EO_{106}PO_{70}EO_{106}$, Mv=12600) was purchased from Sigma-Aldrich. Tetrafluoroterephthalic acid, tetrafluoroterephthalic acid ($H_2BDC\text{-}F_4$, ⩾98%, HPLC), 2-hydroxyterephthalic acid (⩾98%, HPLC) were purchased from damas-beta. Hydrochloric acid (HCl, 36-38 wt%), acetic acid (AR) were purchased from Shanghai Chemical Corp. Zirconium chloride ($ZrCl_4$), furfural (RG, 99%), furfuryl alcohol (RG, 99%), methanol (AR, ⩾99.5%), ethanol (⩾99.7%), isopropanol (⩾99 %), n-butanol (AR, ⩾99.5%), tert-butanol (AR, ⩾99.5%), 1,4-Dioxane (99%) were was purchased Aladdin Chemical Reagent Company. Isopropanol-d_8, D_2O and DMSO-d_6 were purchased from Shanghai Macklin Biochemical Co., Ltd. Commercial ZrO_2 ($cZrO_2$) was purchased from Shanghai Chemical Corp. All reagents and solvents were used directly without any further purification.

Characterization.

The morphologic structures of samples were observed using scanning electron microscopy (SEM, TESCAN/MAIA3, Czech) and Transmission electron microscopy (TEM, JEM–2100F). X–ray diffraction (XRD) spectra were collected on a Rigaku Miniflex diffractometer using Cu–Kα as a radiation source (λ = 0.154 nm). The N_2 sorption was carried out with Quantachrome Autosorb-iQ to measure Brunauer-Emmett-Teller (BET) surface area and pore size distribution. The Brunauer-Emmett-Teller (BET) method was employed for the determination of the specific surface area of the catalysts and the Barrett-JoynerHalenda (BJH) model was employed to analyze the pore size distribution and pore volume. The XPS spectra were investigated using an Escalab 250Xi equipped with Al K radiation. The temperature–programmed desorption of NH_3 (NH_3–TPD) experiment was performed on the BELCAT–B analyzer to determine the acid properties of samples. Approximately 40 mg of the sample was loaded into a U-shaped tube and pretreated at 200 °C under a He flow (50 mL/min) for 1 hour. After cooling to 50 °C, the sample was saturated with a 10% NH_3/He mixture. Subsequently, physically adsorbed NH_3 was removed by purging with He at 50 mL/min for 1 hour. Finally, the temperature was increased to 800 °C at a ramp rate of 10 °C/min under the same He flow, and the desorbed NH_3 was monitored by a thermal conductivity detector (TCD). Fourier transform infrared spectroscopy (FTIR) was collected by a Nicolet 7000–C spectrometer using the KBr disc method. The FTIR spectra of pyridine adsorption were measured at 150 °C using an EQUINOX-55. Thermogravimetric analysis (TGA) was performed using a 209F1 Libra instrument under aerobic circumstances at a heating rate of 10°C/min (flow rate of 20 mL min^{-1}). The FTIR spectra of pyridine adsorption were measured at 200 °C using an EQUINOX-55. The Zr in reaction solution was measured using ICP-OES (Prodigy-ICP).

NMR determination was performed on nuclear magnetic resonance (NMR, 400 MHz) equipment. The experiment details of Figure 5c: The IPA reaction solvent was also qualitatively determined by ^1H nuclear magnetic resonance (NMR, 400 MHz) with

using D_2O as a solvent. The reaction mixture containing different catalysts in isopropanol was allowed to react at 170 °C for 4 h. After cooling, a 100 μL aliquot was taken and diluted with 0.5 mL of D_2O for direct measurement. Qualitative determination of the reaction solution: 20 μL of the reaction solution was diluted with 0.5 mL of D_2O and then analyzed by ^{1}H NMR, ^{13}C NMR, ^{19}F NMR spectroscopy. Reaction conditions: 20 mg of catalyst, 2 mmol of FFA, 15mL of IPA, 170℃, 1h, 900 rpm.

Catalytic performance tests

The hydrogenation of furfural (FFA) was performed in a sealed stainless-steel batch reactor equipped with magnetic stirring. In a typical experiment, 50 mg of catalyst and 1 mmol of FFA were dispersed in 15 mL of isopropanol. The reactor was then brought to the desired reaction temperature. Following the reaction, the mixture was filtered, and the resulting liquid phase was characterized using gas chromatography–mass spectrometry (GC–MS, Agilent 8860 GC coupled with 5977B MS). Catalyst durability was evaluated through consecutive reaction cycles. After each run, the solid catalyst was separated via centrifugation, rinsed thoroughly with isopropanol, dried, and subsequently reused under identical conditions.

Calculation details

Density functional theory (DFT) calculations were conducted using the Vienna Ab initio Simulation Package (VASP, version 6.3.2). The electron–ion interactions were treated within the projector augmented wave (PAW) framework, while exchange–correlation effects were described by the generalized gradient approximation (GGA) with the Perdew–Burke–Ernzerhof (PBE) functional. A kinetic energy cutoff of 450 eV was adopted for the plane-wave basis set. Geometry optimizations were performed until the total energy variation was less than 10^{-5} eV and the residual forces on each atom were below 0.02 eV $Å^{-1}$. To avoid spurious interactions between periodically repeated slabs, a vacuum layer of 15 Å was applied along the z direction. The Brillouin zone

integration for slab models was carried out using a 2 × 2 × 1 Monkhorst–Pack k-point mesh.

Method

Calculation method of defect amount of mUiO-66

The detail number of linker deficiencies per Zr^6 formula unit (x) is calculated by the following:

$$W_{t.}PL_{pre} = \frac{(W_{pre} - W_{end})}{NLpre} \quad (1)$$

$$NL_{exp} = (6 - x) = \frac{W_{pre} - W_{end}}{W_{t.}PL_{pre}} \quad (2)$$

$$x = 6 - NL_{exp} \quad (3)$$

where: W_{end} is the end weight of the TG trace (normalized to 100%), W_{pre} is the theoretical weight of the dehydroxylated mUiO-66 ($Zr_6O_6(BDC\text{-}F_4)_6$: 2059.79 g/mol), $W_{t.}PL_{pre}$ is a value for the theoretical weight loss per BDC-F_4 linker, 6 is the number of linkers in the ideal Zr-oxo unit, NL_{exp} is the number of BDC linker in experiment.

Calculation method of TON and TOF

$$n_{active\ sites} = n_{Total\ acid\ content} \times m_{catalyst} \quad (4)$$

$$TON = \frac{n_{FOL}}{n_{active\ sites}} \quad (5)$$

$$TOF = \frac{TON}{t} \quad (6)$$

where: the number of active sites ($n_{active\ sites}$) was estimated from the total acid content determined by NH_3-TPD, multiplied by the mass of catalyst ($m_{catalyst}$) used. The turnover number (TON) was then calculated as the molar ratio of furfuryl alcohol (FOL) produced to the active sites. The turnover frequency (TOF) was obtained by dividing the TON by the reaction time (t) in hours. This calculation assumes that each NH_3 molecule titrates one accessible Lewis acid site under the measurement conditions.

Supporting Figures

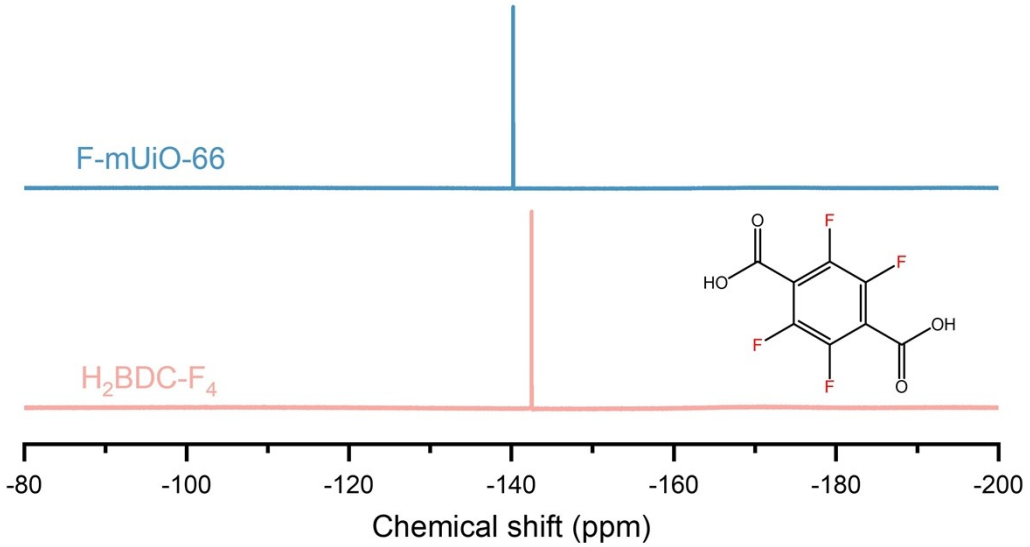

Figure S1 ^{19}F NMR of decomposed F-mUiO-66 and $H_2BDC\text{-}F_4$.

The clear digestion of mUiO-66 in a D_3PO_4/D_2O mixture and the D_2O solution of the $H_2BDC\text{-}F_4$ salt were analyzed by ^{19}F NMR spectroscopy. A distinct fluorine signal was observed for the digested mUiO-66 sample. Together with the EDS result, the ^{19}F NMR data provide compelling evidence for the successful synthesis of the MOF framework. Of note, the slight difference in chemical shift between $H_2BDC\text{-}F_4$ and mUiO-66 is attributable solely to the use of different deuterated solvents and does not affect the conclusion.

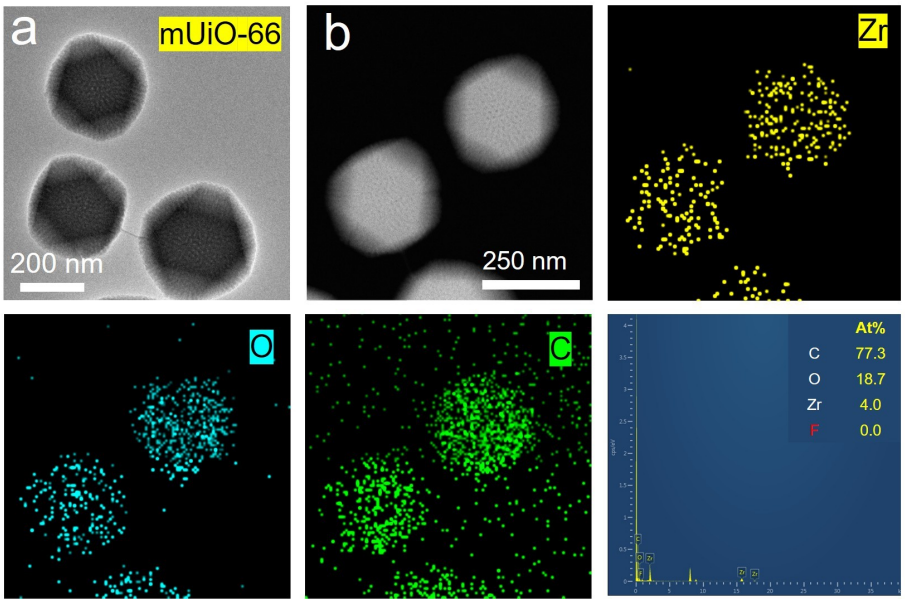

Figure S2 (a) The TEM, (b) HAADF-STEM image and corresponding EDS maps of prepared mUiO-66.

Figure S3 Scale-up synthesis of F-mUiO-66.

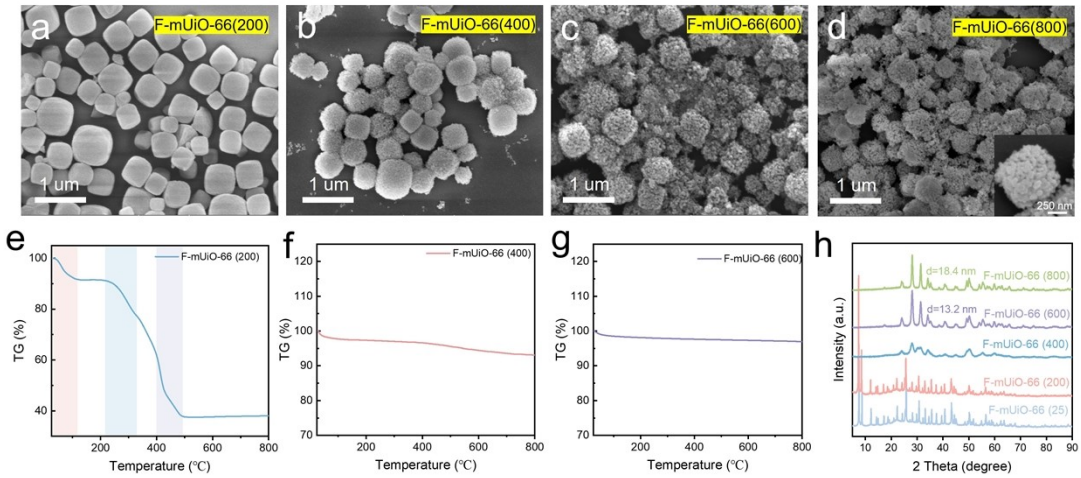

Figure S4 SEM images of F-mUiO-66 pyrolyzed at different temperatures; (a) 200°C, (b) 400°C, (c) 600°C, (d) 800°C and (e-g) their TG curves under air atmosphere and (h) XRD patterns.

SEM images (Figure S3 a-d) revealed the gradual decomposition of the F-mUiO-66 framework with increasing calcination temperature, accompanied by progressive pore enlargement. TG analysis (Figure S3 e-g) showed that the organic framework content decreased continuously and was completely removed at 600 °C. XRD patterns (Figure S3 h) confirmed the gradual transition from F-mUiO-66 to pure ZrO_2. Notably, when the calcination temperature reached 800 °C, further grain growth of ZrO_2 was observed, which likely traps more active sites within the bulk phase, rendering them inaccessible for catalysis.

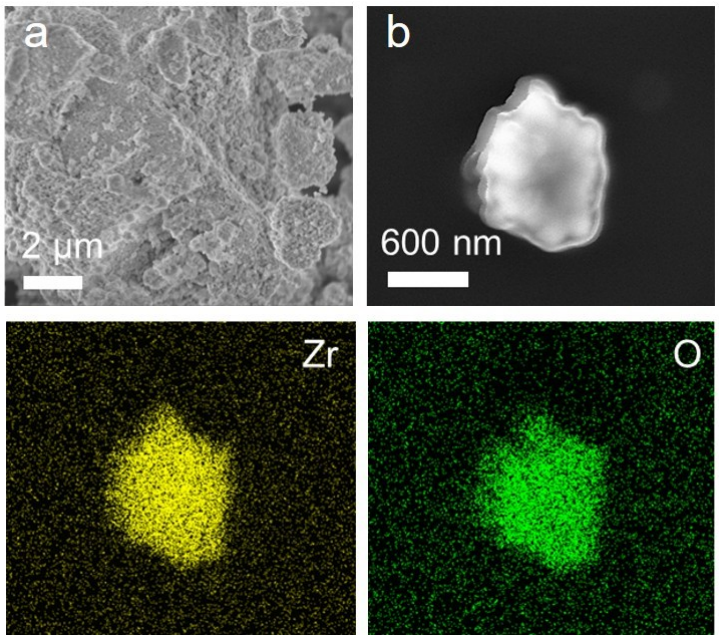

Figure S5 The SEM images and corresponding EDS maps of $cZrO_2$.

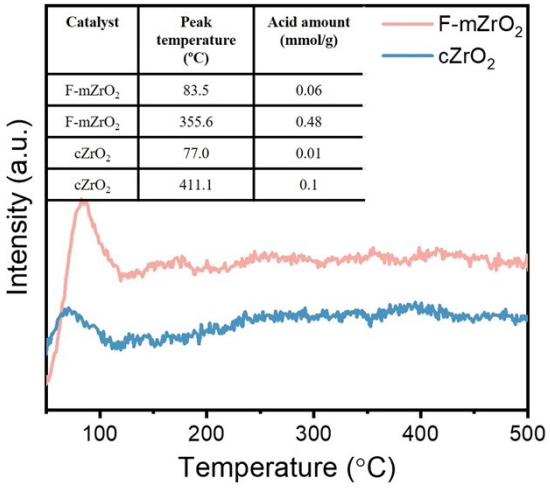

Figure S6 NH_3–TPD and total acid amount profiles of F-modified mesoporous zirconium oxide (F-$mZrO_2$) and commercial zirconium oxide ($cZrO_2$) catalysts.

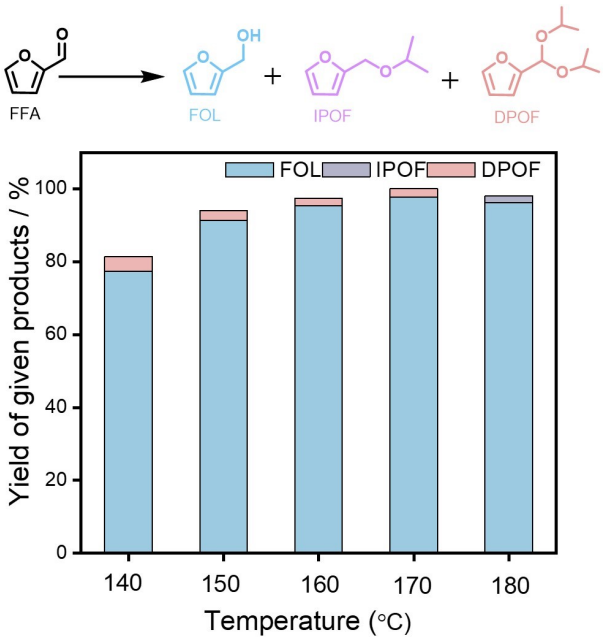

Figure S7 FFA conversion and product distribution over F-ZrO_2 and cZrO_2 catalysts under 140-180 °C.

As the reaction temperature increases from 140 to 170 °C, the yield of FOL over F-mZrO_2 rises sharply and ultimately reaches an impressive 97.8%. When the temperature is further elevated to 180 °C, the produced FOL undergoes secondary acetalization with isopropanol, forming IPOF as a byproduct.

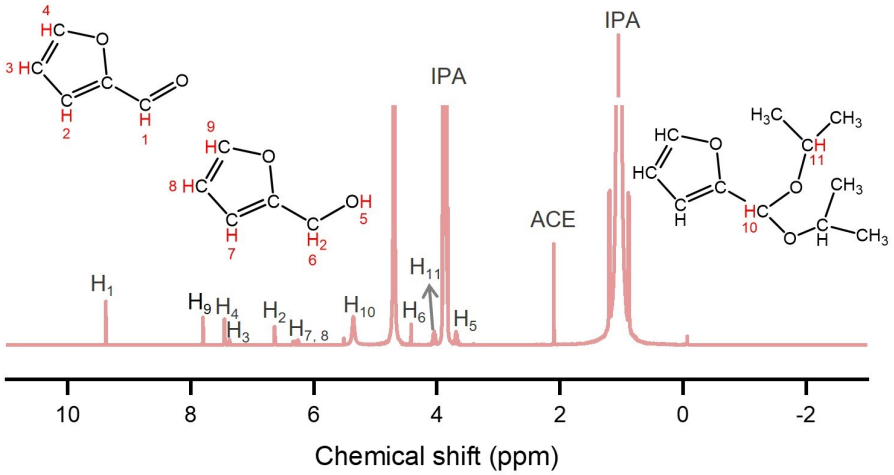

Figure S8 ^1H spectrum of reaction solution; Reaction conditions: 20 mg of catalyst, 2 mmol of FFA, 15mL of IPA, 170℃, 1h, 900 rpm. This spectrum is provided as

supplementary information to illustrate substrate conversion and product formation during the reaction process.

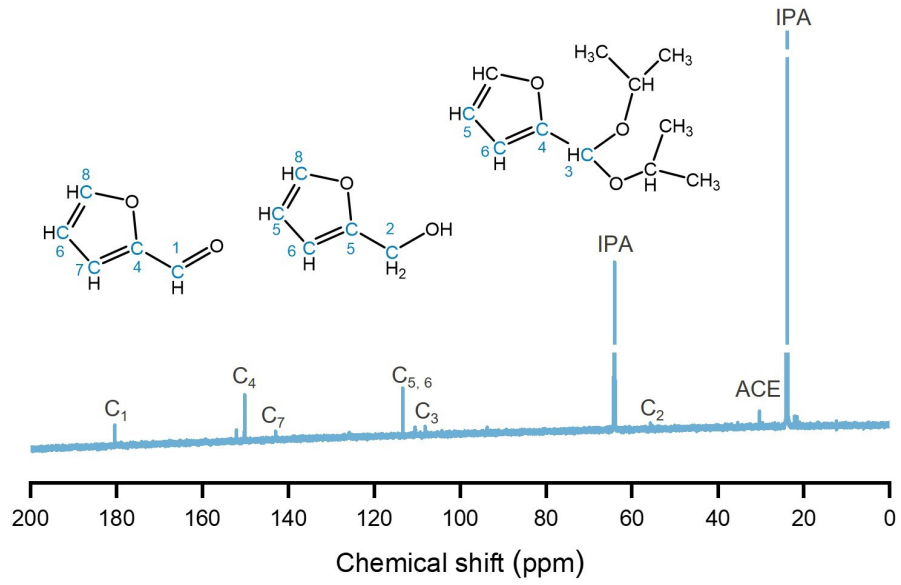

Figure S9 ^{13}C spectrum of reaction solution; Reaction conditions: 20 mg of catalyst, 2 mmol of FFA, 15mL of IPA, 170℃, 1h, 900 rpm. This spectrum is provided as supplementary information.

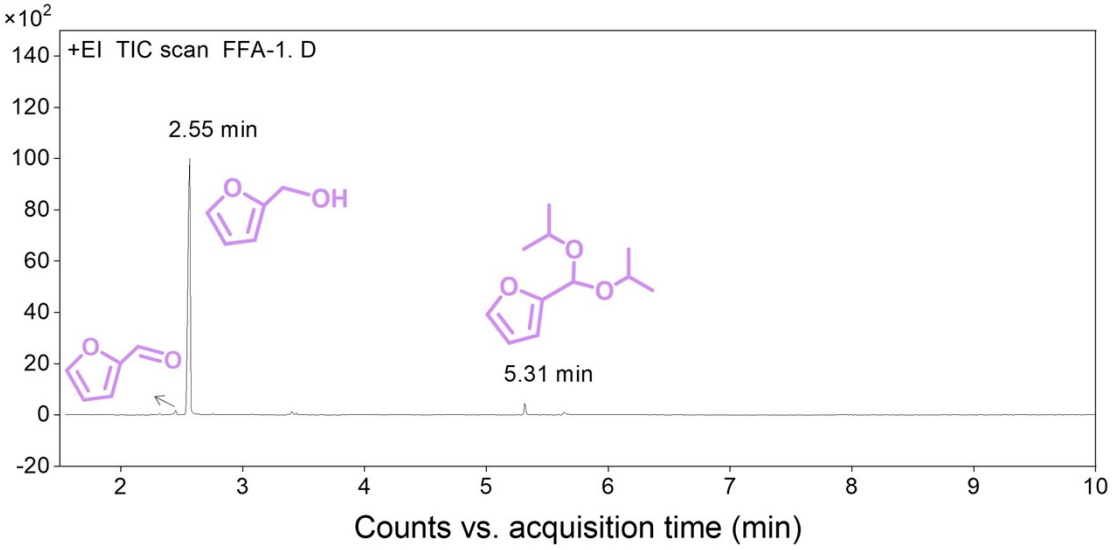

Figure S10 Chromatograms of products distribution of furfural transfer hydrogenation F-mZrO_2 catalyst. Reaction conditions: 50 mg of catalyst, 1 mmol of FFA, 15mL of

IPA, 170℃, 4 h, 900 rpm.

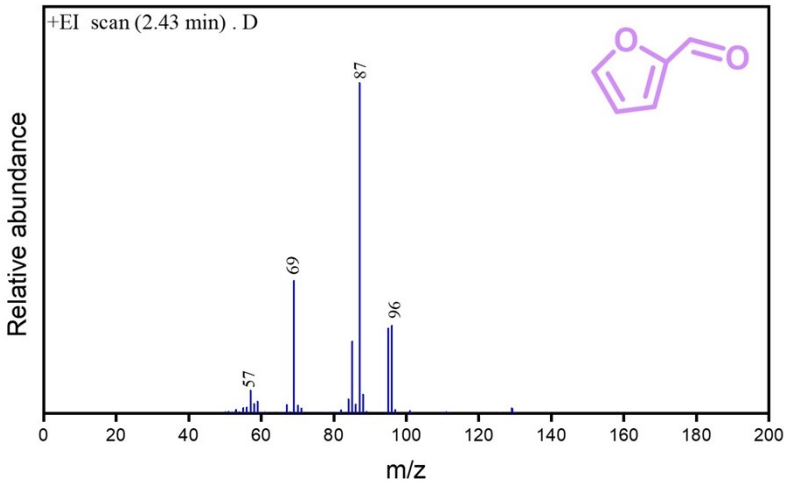

Figure S11 The mass pattern of furfural substrate.

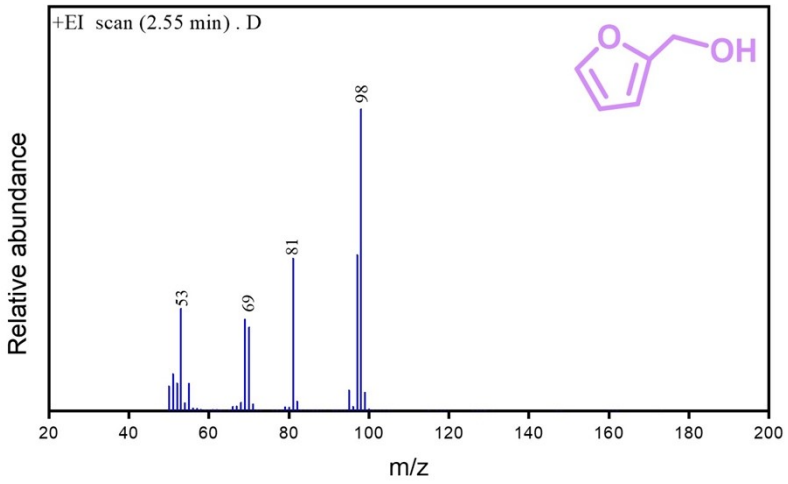

Figure S12 The mass pattern of furfuryl alcohol product.

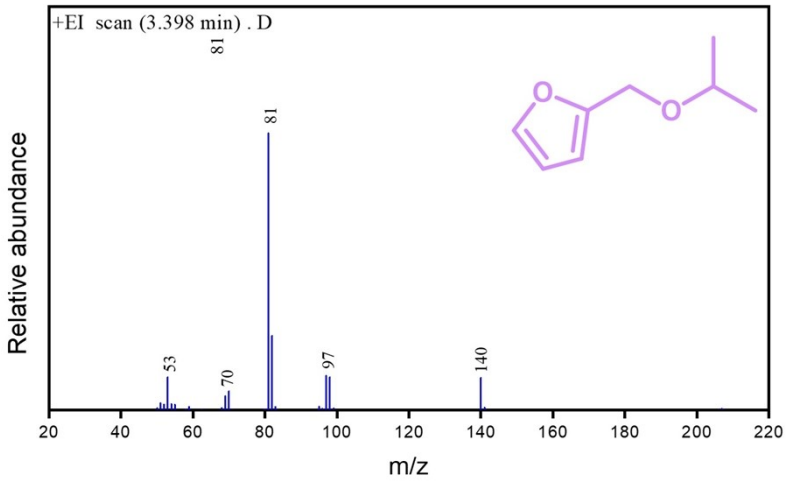

Figure S13 The mass pattern of furfuryl alcohol product.

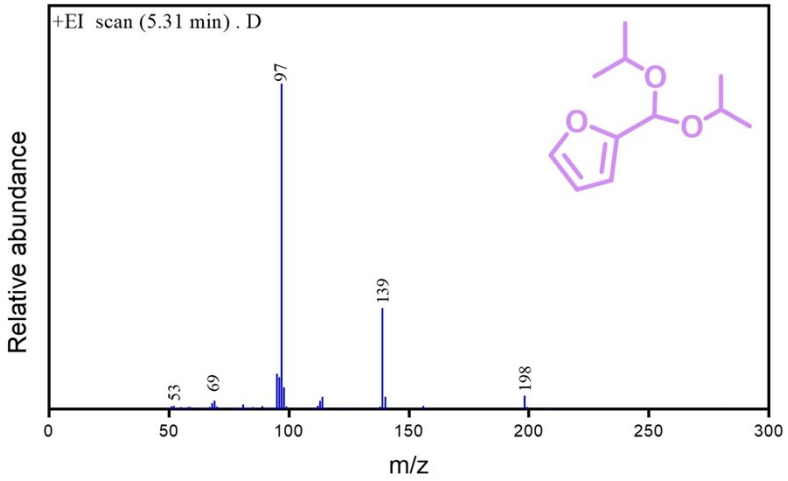

Figure S14 The mass pattern of DPOF by-product.

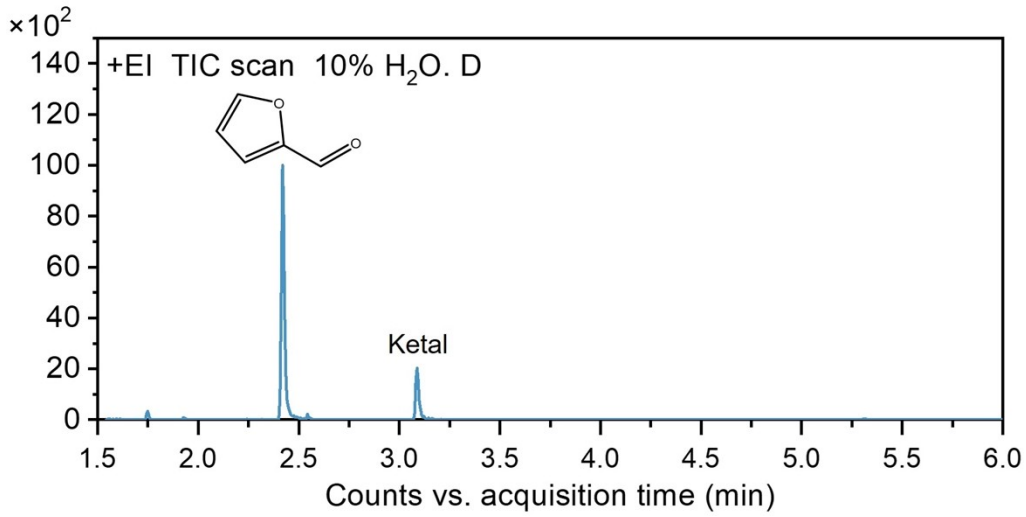

Figure S15 Chromatograms of products distribution of furfural hydrogenation using water as a co-solvent.

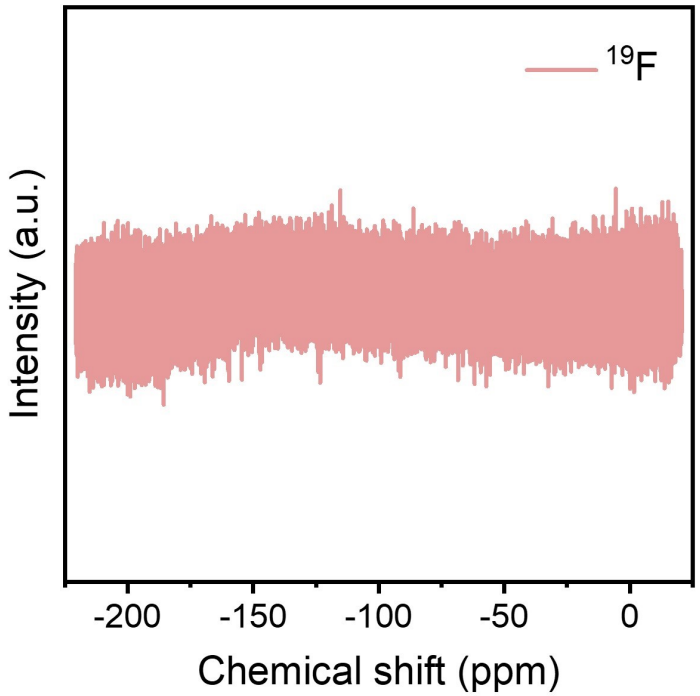

Figure S16 ^{19}F spectrum of reaction solution; Reaction conditions: 20 mg of catalyst, 2 mmol of FFA, 15mL of IPA, 170°C, 1h, 900 rpm.

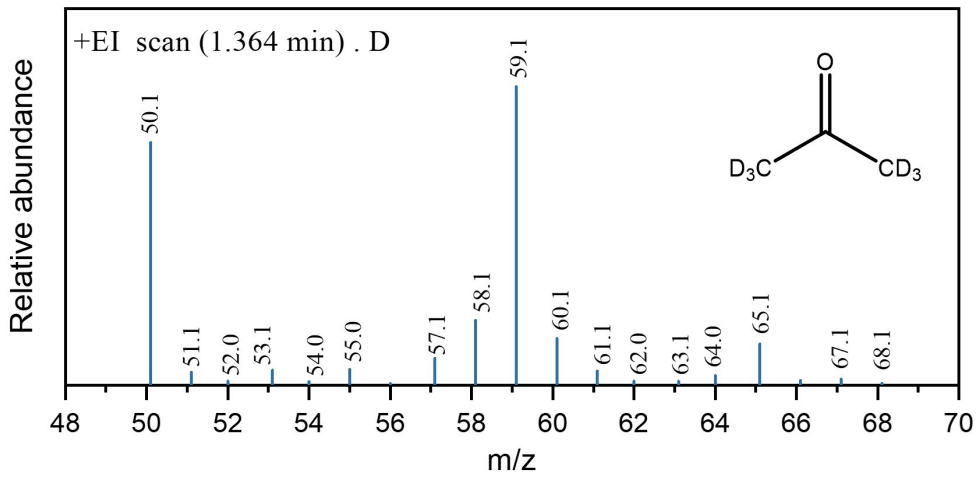

Figure S17 The mass pattern of CD_3COCD_3. Reaction conditions: 50 mg of catalyst, 1 mmol of FFA, 15mL of 1,4-Dioxane, 200 mg IPA-d_8, 170℃, 4 h, 900 rpm.

To further confirm the coupling between isopropanol dehydrogenation and furfural hydrogenation, we performed additional isotope labeling experiments analyzed by GC-MS. In this experiment, 200 mg IPA-d_8 was used as the hydrogen donor and 1,4-Dioxane as solvent. After the reaction, the liquid phase was analyzed by GC-MS. As shown in Figure S16, the mass spectrum of the product fraction exhibited a clear molecular ion peak at m/z = 65.1, which is characteristic of perdeuterated acetone (CD_3COCD_3). Of note, the purities of furfural and isopropanol used in this work are both above 99%, and no reaction occurred when water was employed as a co-solvent, which completely rules out any contribution from protons provided by water in the system. Combined with the observation of deuterated furfuryl alcohol ($[M+1]^+$ peak at m/z = 99), provides direct and unambiguous evidence that the hydrogen transfer proceeds via a coupled pathway, which strongly supports the proposed MPV mechanism.

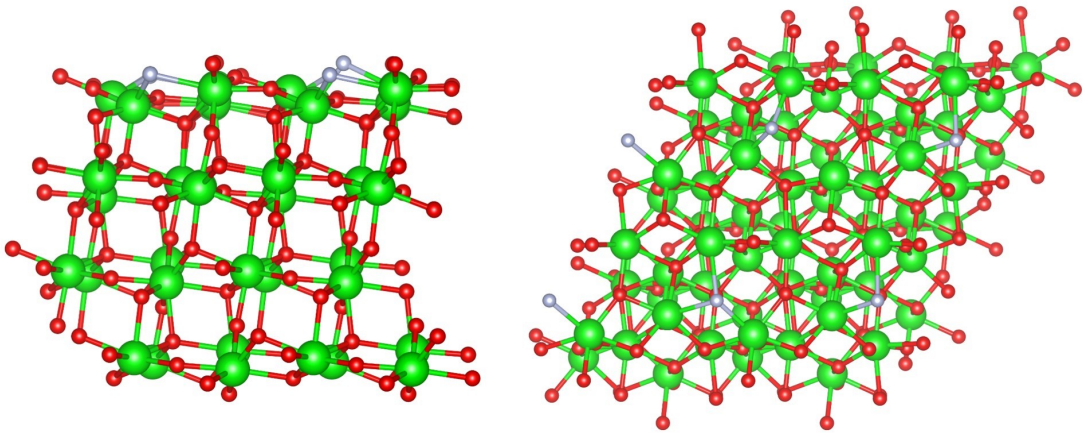

Figure S18 The optimized structures of F-mZrO_2.

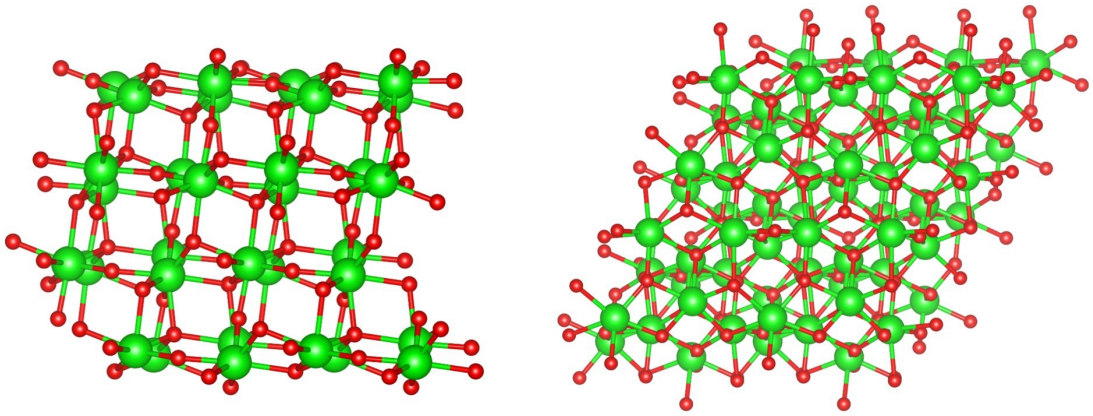

Figure S19 The optimized structures of mZrO_2.

Supporting Table

Table S1 Catalytic hydrogenation of different carbonyl compounds over the as-prepared F-mZrO_2 catalyst [a].

Entry	Substrates	Products	Con./%	Sel./%
1	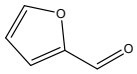	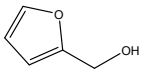	100	97.8
2	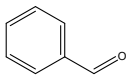	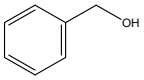	84.3	94.1
3	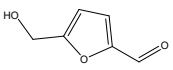	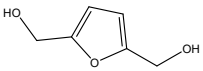	81.3	95.6

[a] Reaction conditions: 50 mg of catalyst, 1 mmol of substrates, 15 mL of IPA, 170 °C, 4 h, 900 rpm.

Product identification and quantification were performed by GC–MS. For 5-Hydroxymethylfurfural system with high boiling point, HPLC with an authentic standard was employed.

The FFA hydrogenation of a series of compounds containing carbonyl groups was also investigated to verify the applicability and feasibility of the F-mZrO_2 catalyst. As shown in Table S1, in all cases, conversions above 80% are achieved and selectivities towards the target products are more than 90%. The results further reflect its potential applications of F-mZrO_2 catalyst in the efficient exploitation and utilization of biomass-derived compounds.